Kuwait J. Sci. Eng. **36** (2B) pp. 1-93, 2009

Effect of chromizing on bonding mechanism of a sheet composite of Brass-Steel-Brass

BEHZAD TOLAMINEJAD*, HOSSEIN ARABI*

School of Materials Science and Engineering, Iran University of Science and Technology, Narmak-Tehran-Iran, btolaminejad@iust.ac.ir and Center of Excellence of Advanced Materials and Processing, CEAMP.

ABSTRACT

This article describes the effects of roll bonding on bond strength of a sheet composite produced from MS90 (*CuZn*10) alloy strips and hard chromized *St*13 steel sheets. Hard chromium applied on the surface of steel sheets acted as joining interlayer. It was found that the joining between these two metals resulted from two different types of bonds: block bonds, between the MS90 strips and the fragmented chromium topcoat layer, and blank bonds, between the MS90 and bare steel surface within the area of the fragmented chromium coating. In addition, the effects of plating time on the thickness of the coating layers which resulted to different area fraction of blank bond during rolling and consequently affected the bond strength of the sheet composite was investigated. Reducing the initial strip thickness and doing annealing heat treatment after rolling can effectively improve the bond strength. A linear relationship observed between the overall bond strength and the area fraction of blank bonds.

Keywords: Roll Bonding, Hard Chromizing, Brass-Steel-Brass Composite, Bonding Mechanism.

INTRODUCTION

Cold roll bonding process take place at room temperature (Granjun 1991, Thomas & Petri, 1994). It has been reported (Kreye & Thomas 1977, Bay 1986) that the lack of any evidence of solidified liquid on the cast structure of the interface is an indication that no liquid phase can be formed on the interface and therefore a direct bond emerges in the solid state. The plastic deformation due to the external pressure applied on the interface zone provides the activation energy for cold roll bonding (Granjun 1991, Thomas & Petri, 1994). Roll bonding is a process for establishment of atom- to - atom bond between two pieces to be joined through intimate contact of their contamination free surfaces (Vaidyanath et al. 1959, Cave & Williams 1973, Wright et al. 1978).

During the last three decades, the production of sandwich strips by rolling process, which is a more efficient and economical approach compared to other

types of processes, has become an increasingly important subject of study among researchers (Hwang et al. 1995, Butlin & Mackay 1979). Recently, in addition to various analytical researches into the multi-layered composites (Al-Sharee dah, 2008, Hwang et al., 1995, Kang & Kwon, 2002), there are several experimental investigations carried out on different materials. Bimetallic sheets and strips of steel and copper alloys are among the most successful types of laminated composites in use because of the comprehensive properties derived from the component materials. However, it is said (Pan et al. 1989) that the existing cold rolling technique for production of bimetal of copper alloy strips and steel sheets required at least nearly 70% thickness reduction to ensure relatively acceptable bonding, though the strength of these bonds are still low.

Annealing heat treatment of these types of sheet composites offers a promising solution for stronger bonding. On the other hand, since strain aging of steel is caused by the presence of interstitial carbon and nitrogen (Danesh Manesh & Karimi Taheri 2003), they can deteriorate the ductility due to formation of cottrel atmospheres and dislocation locking. Therefore, multi-layered composites must be annealed to develop a high formability for the next deep drawing operation. However, the original fragile oxide layer on the surface of steel sheets can prevent the development of a strong bond during annealing. Therefore, in order to prevent surface oxidation, electro plating technique is widely used. This provides less contaminated virgin metal at the surfaces to be jointed. On the other hand, one should notice that the effect of fragmentation types of different coatings during roll bonding on the strength of the produced composite is different. One of the differences occurs during fragmentation of different types of coating is surface fraction of the virgin metal expose at the intimate surfaces. Indeed, when the surface is electroplated with brittle coating; this coat can not keep its continuity with the ductile material at interface due to their modulus differences (Hwang et al. 1995, Karimi Taheri 1993), hence it becomes fragmented during cold rolling. The distances and dimensions of fragments depend on the ductility of the material and the coating surface expansion under different amounts of rolling thickness reduction applied. According to Fig. 1, the upper soft sheet has two deformation zones; Zone I (EBCF) is mainly extruded into the gap provided by fragmentation of coating and the material in zone II (AEFD) moves downward, towards the hard base metal sheet. During deformation, two dead zones along AB and DC with α angle will be produced. If the dimension ratio of the fragments t/w (i.e., thickness to width ratio) be small, it is said (Zhang & Bay 1986) that the amount of material extruded through the space (i.e., materials in zone I) would not reach a steady state situation, and therefore the chance of establishing a strong bond will be diminished. Whereas, when the dimension ratio (t/w) is large enough, the extrusion of material in zone I will become complete, so that it reaches a steady state condition and the dead

zones in zone II disappear. In the present research, a novel mathematical model was proposed for rolling a tri-layer composite, so that by using this model, one can predict the strengthening mechanisms of bonding via microstructural observation and tribological behavior of interface region.

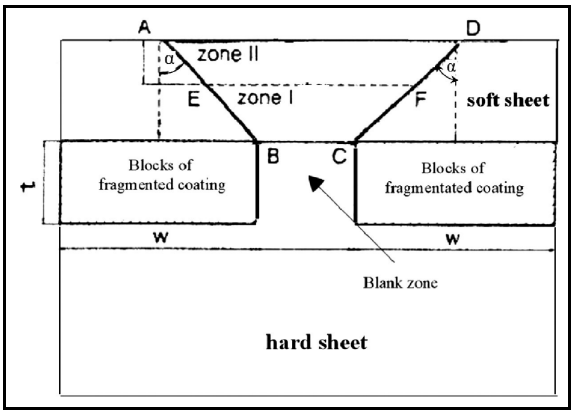

Figure 1. Geometry of the deformation zone of extrusion through cracks at interface (Zhang & Bay 1986)

Accordingly, the main objective of this study was to determine the factors influencing the bonding strength of the bimetallics composite formed by rolling MS90 alloy strips and hard chromized steel, study their mechanism of interface bonding and on that base an experimental model was developed. So, to reach this objective, the following experimental procedure was designed and performed.

EXPERIMENTAL

Fabrication of MS90 alloy strip and hard chromized steel sheets

The brass bars with the composition (in wt%) Cu-10.2% Zn-0.07% Fe-0.05% Pb, was charged into a crucible, kept in a resistance-heated vertical muffle furnace. When the melt reached 1100°C, the furnace was switched off, the crucible was taken out of the furnace, and the agitated melt poured into a steel mold. The cylinder ingot obtained was then extruded into strips of width 45 mm and thickness 0.4 mm at 800°C. A St13 steel sheets, of the composition (in wt.%) Fe-0.54 C-0.35 Mn-0.022 P-0.0014 S, were cut into strips having dimensions of 75×50mm prior to chromizing its surfaces in order to produce a satisfactory sound metallurgical bond (Clemensen & Julstarp 1986). The sheets were then degreased, rust removed and fluxed. After being rinsed with deionized water, the steel specimens were immersed in a chromium plating bath containing Pb-2.5%Sb

anode, $300g/l$ of chromic trioxide, $3g/l$ of sulfuric acid at 53°C and 28 A/dm^2 for different times (10-60min). So hard chromium coating layer having various thicknesses (t) were obtained in the chromium bath. The thicknesses of the coating layers were measured using a Nikon light microscope.

The roll bonding of MS90 alloy strip and hard chromized steel sheets

The main steps taken for welding the sheet of MS90 alloy to a sheet of chromized steel by the cold rolling process were as follows:

i - Two strips of MS90 alloy were placed in each surface of the chromized steel strip and aligned as a pack.

ii - A small part of the surfaces at one end of the chromized steel sheet facing the MS90 alloy strips were then smeared with graphite in order to prevent bonding between the edges of the strips during rolling.

iii - The pack was cold rolled in different thickness reduction (R_t) to produce a metallic sheet composites (Fig. 2).

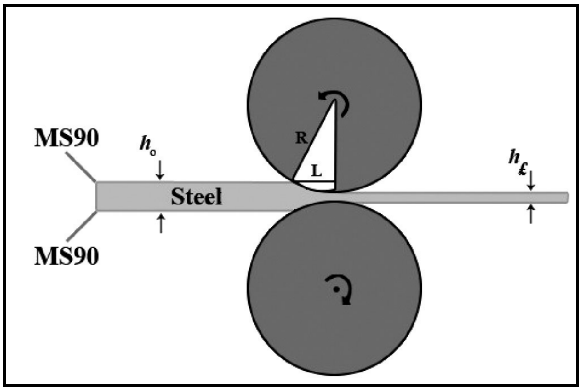

Figure 2. Schematic of cold roll welding of MS90/St13/MS90 pack

Worth mentioning that for roll welding the strips of copper alloys and steel, a rolling pressure range of 1000 - 3400 MPa and a threshold reduction range of 40 - 80 percent have been reported (Thomas & Petri 1994, Tylecote 1968). The amount of threshold reduction for joining the sheet metals is said to be (Cave & Williams 1973) greatly depended on the surface treatment and the magnitudes of the rolling parameters such as diameter, rigidity and surface roughness of rollers, preliminary thickness of each layer before rolling and geometry of deformation zone. A small part of the surface at one end of chromized steel sheet facing the MS90 alloy strip was smeared with graphite to prevent bonding between the strip and the sheet at this particular interface during subsequent rolling. Then, one of the steel sheets was placed in between two MS90 alloy

strips, and rolled together with no lubricant using a laboratory rolling mill with a loading capacity of 15tons. The roll diameter was 170mm, and the rolling speed was 5rpm (44.48 m/s). The initial thickness of the sheets with a constant clad ratio in addition to thickness reduction and annealing conditions of this study are shown in Table 1.

Table 1. The conditions of roll bonding experiments.

Initial thickness of sheets	Thickness reduction	Annealing conditions after bonding
St13(5mm) , MS90(0.8mm)	49,54,60,63	----------
St13(5mm) , MS90(0.8mm)	49,54,60,63	700^{O}C , 30 min
St13(2.5mm) , MS90(0.4mm)	40,44,49,54,60,63	----------
St13(2.5mm) , MS90(0.4mm)	40,44,49,54,60,63	700^{O}C , 30 min
St13(1.25mm) , MS90(0.2mm)	31,36,40,44,49,54,60,63	----------
St13(1.25mm) , MS90(0.2mm)	31,36,40,44,49,54,60,63	700^{O}C , 30 min

The bond strengths of the sheet composites were measured using the peeling test according to ASTM-D903-93. The breaking off forces in the peeling tests were measured as follows:

$$AveragePeelStrength = \frac{AverageLoad}{BondWidth} \tag{1}$$

The average load was measured from the graph of peeling force versus peeling distance. A typical graph for measuring the average peeling strength for a constant bond width of 40mm is presented in Fig. 3.

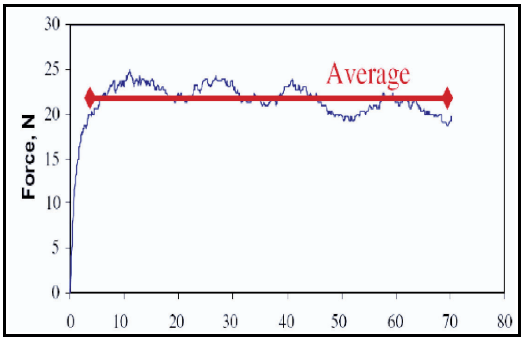

Figure 3. Typical graph of the peeling force versus peeling distance used for calculation of average peeling force.

The peeling test was performed using an Instron tensile testing machine with 1 KN load cell. The mean bonding strength was measured by a peeling test machine illustrated in Fig. 4. A crosshead speed of 5 mm/min was used in the tests. The sensitivity of the load cell was 0.1 N.

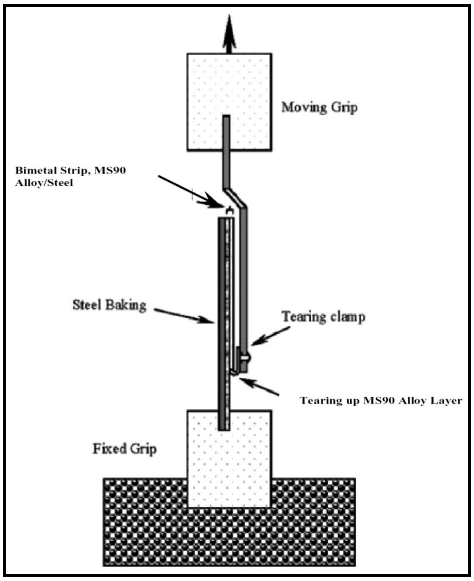

Figure 4. Configuration of peeling test used in this investigation.

To determine the microstructure of the tri-layer composite after deformation and the interfaces of the metal sheets, polished samples were etched first with 3% nital and then in a solution of 25g $FeCl_3$, 20ml HCl, 100ml H_2O. Also, after peeling tests the fracture surfaces were cleaned thoroughly by acetone in an ultrasonic stirrer. Then a JEOL model 5910 LV scanning electron microscope (SEM) was used for fractography study.

RESULTS

Following the chromizing of the St13 steel surfaces at 53°C for various times, the thickness of chromized layers were measured at various cross section areas to obtain the mean value of the chromium layer for each dipping time. The results of this measurement are presented in Fig. 5. This figure shows that by increasing the dipping time, the thickness of the hard chromium layers increased. A semi-parabolic relationship between thickness and dipping time, similar to those obtained by other researchers (EI-Mahallawy et al. 1997, Yongbing et al. 2000) can be observed.

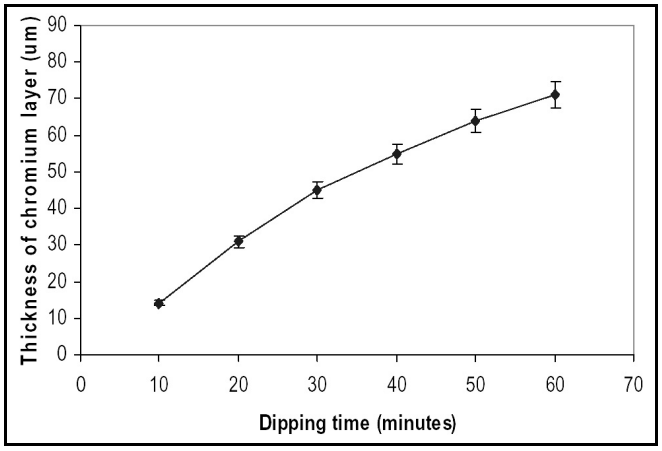

Figure 5. Variation in the thickness of the coating layer with dipping time

Variation of bond strength of the MS90-St13 sheet composites having constant thicknesses of 0.2, 1.25mm and various hard chromium interlayer thicknesses is presented in Fig. 6. The threshold deformation for formation of roll bonding was about 36%. The bonding strengths of the MS90/steel specimens up to a total thickness reduction of 49% increased with increasing the thickness of the coating up to 55 m then decreased slightly for the thickness more than 55 m. However, for the total reduction range of 54% - 63%, the peeling strengths increased with increasing the thickness of hard chromium.

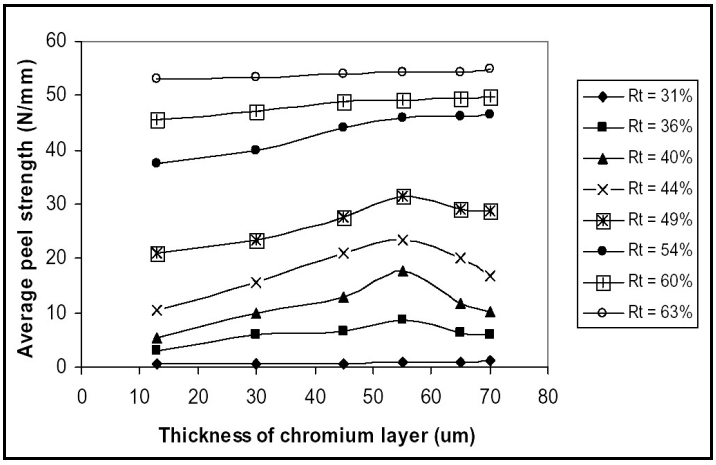

Figure 6. Variation of the bond strength with thickness of the coating layer for different thickness reductions.

This figure also indicates that for the total reduction of 63%, increasing the thickness of chromium layer did not affected the peeling strength and this strength seems to be independent of the thickness of the hard chromium interlayer. Also, Fig. 7 presents the effect of initial thickness of sheets on the bond strength of sheet composites. This figure demonstrates that by decreasing the initial thickness of both MS90 brass and St13 steel sheets, the bond strength increases while the threshold thickness reduction decreases for different thicknesses of chromium layer. Meanwhile, according to Fig. 7, the sample subjected to annealing heat treatment had the highest bonding strength for any thickness reduction in comparison to bonding strength of other samples.

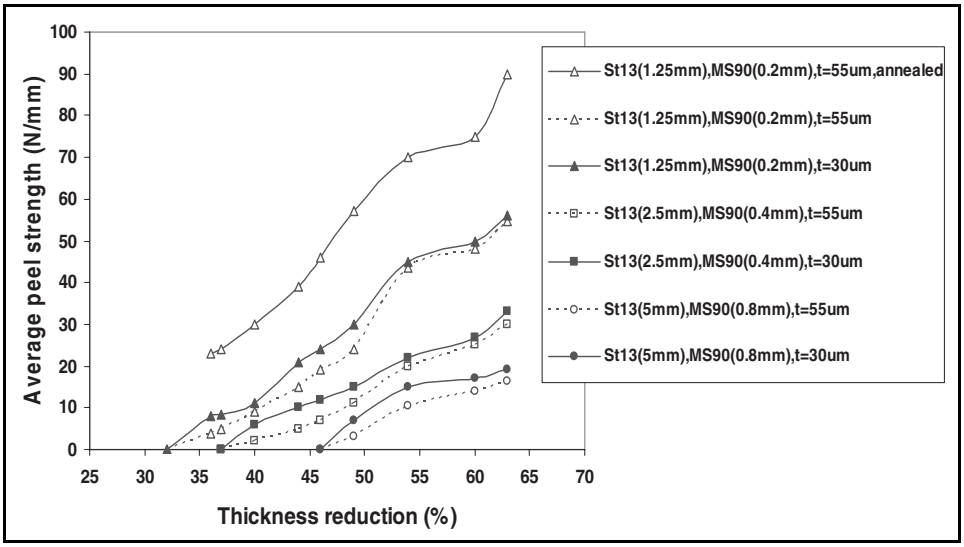

Figure 7. Effects of initial thickness of the sheets, total thickness reduction and chromium coating thickness on bond strength of MS90/St13.

Fig. 8 shows a typical sections of bonded MS90 alloy/chromized St13 steel sheet at three different thickness reductions (36, 54 & 60%) and also two different chromium layer thicknesses (30, 55μm). It is clear from this figure that the coating layer was broken into fragments which get away from each other by further reductions. These fragments (termed blocks) rotated along the deformation stream lines during rolling. The amount of rotation of blocks increased with the increase of the total thickness reduction and the areas between any two blocks (termed blanks) also decreased with increasing the amounts of blocks rotation.

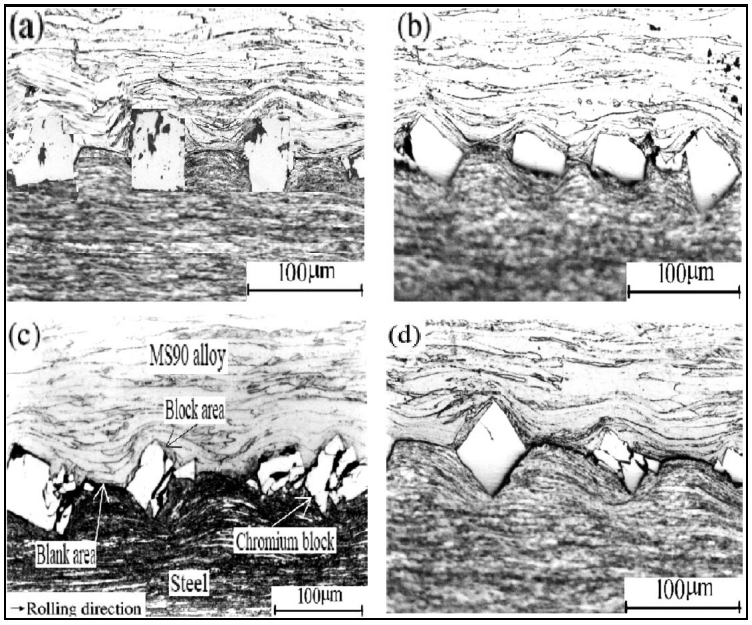

Figure 8. Microstructures of the bonded interfaces of MS90/chromized St13 steel composite sheets produced by (a) total reduction(R_t) 36%, showing un rotated chromized blocks with an average thickness(t) 55μm; (b) Rt = 54% and t = 30μm; (c) R_t = 54% and t = 55μm; (d) R_t = 60% and t = 55μm

The fracture surface of the specimen shown in Fig. 8c is presented in Fig. 9. This figure shows the fractured surface of St13 steel in two different magnifications. The wider blanks were in the direction of rolling all over the surface of the steel substrate and the narrower blanks were perpendicular to the rolling direction.

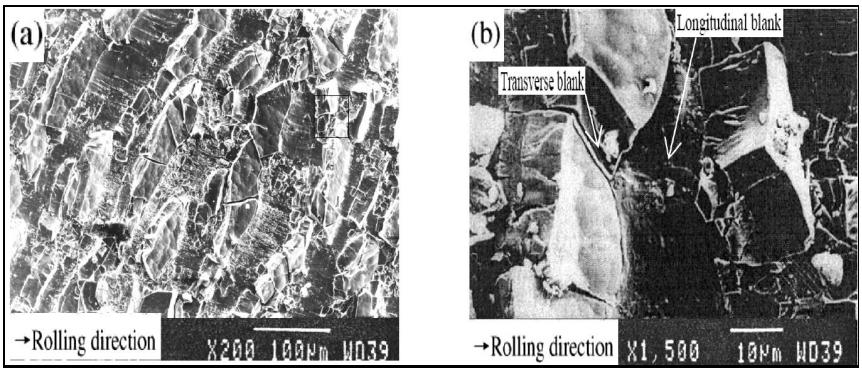

Figure 9. Typical fracture surface of the sheet composite of the specimen shown in Fig. 8c: (a) showing fragmented chromium layers on the steel surface; (b) higher magnification of (a)

Fig. 10b shows the cleavage feature at the steel peeled surface of roll bonded sheets with thicknesses of 5mm. Although there are a little ductile fractures zones within the cleavages zones. On the peeled steel surface of sheets with thickness of 1.25 mm (Fig. 10a), both the ductile and the brittle areas can also be observed, in the same way.

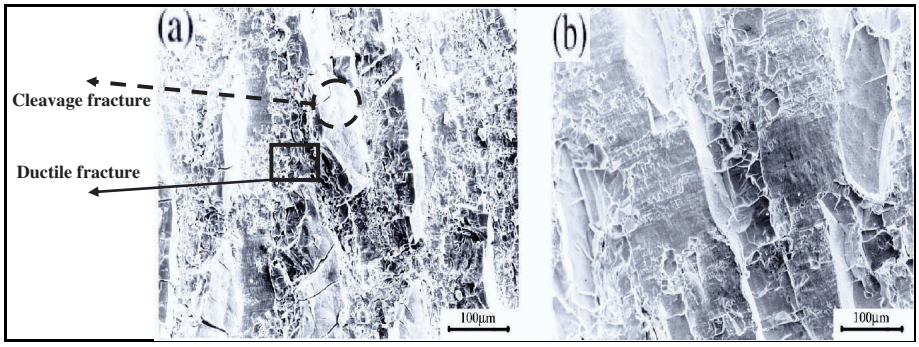

Figure 10. Steel peeled surface of roll bonded MS90/St13 steel alloy strips with different initial thickness (a) 1.25mm, (b) 5mm

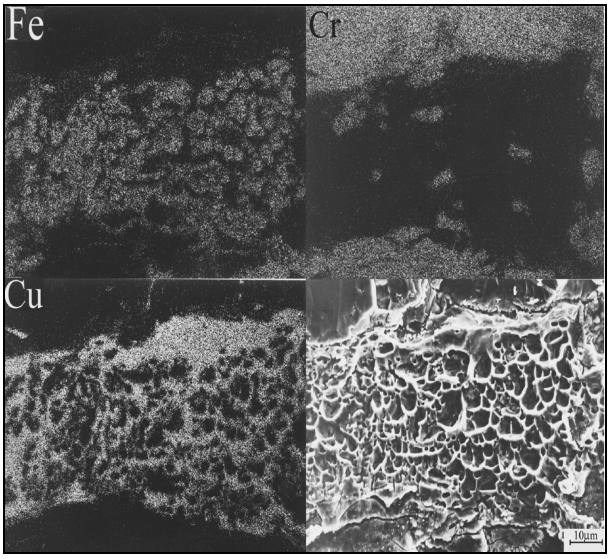

Figure 11. X-Ray Maps taken from the ductile zone of a peeled MS90 surface

X-Ray Maps taken from the matching fractured pair of St13 steel belonging to the specimen having maximum bonding strength is presented in Fig. 11 in higher magnification. The maps show a large amount of Fe in addition to chromium is presented at the surface of the peeled brass sheet.

A longitudinal section of the sheet composite specimen (i.e., Fig. 8c) annealed for 30 minutes at 700°C is presented in Fig. 12. Micrograph in Fig. 12a shows recrystallized grains at both sides of interface and the positions of the un-rotated blocks shown schematically in Fig.12b and that of the rotated blocks in Fig. 12c.

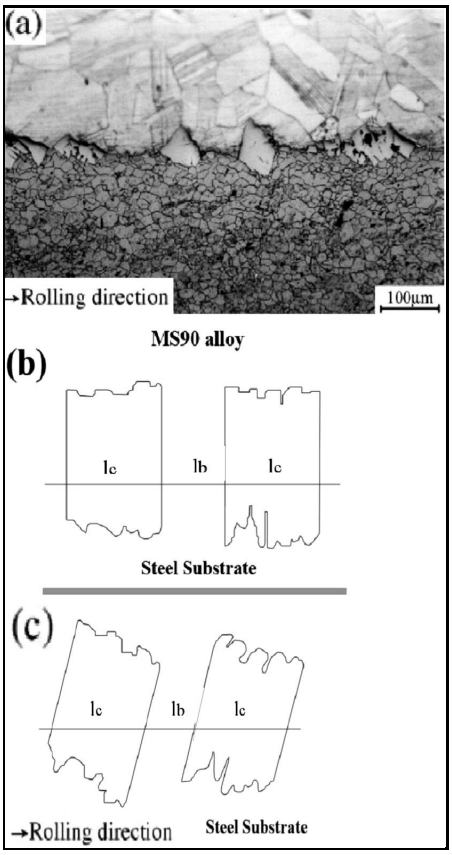

Figure 12. (a) Microstructure of the specimen related to the specimen shown in Fig.(8-c) which annealed for 30 minutes at 700°C; (b) Schematic of the fragmented chromium interlayer blocks before being rotated and (c) decreased in the blank area followed by rotation of chromium blocks

DISCUSSION

The formation of the blanks area was due to the fact that the steel substrate elongated in the direction of rolling, but the chromium layer broke into fragments or small blocks, being unable to elongate along with the steel substrate because of its brittleness, therefore, the movement of these chromium blocks is possible by dragging force due to the flow of metallic layers in rolling direction. The widths of

the blanks areas in rolling direction were much greater than those of the transverse blanks, as shown in Fig. 9. When MS90 alloy strips were extruded into blanks, two different joining mechanisms took place. First, the MS90 alloy was fairly adhesive to chromium block by the geometrical constraints; Second, the MS90 layer was bonded metallurgically to the steel substrate in the blank area. The overall bond strength depended on the strength of both mechanisms, but the effect the blank bond was more than that the block bond. Also, two phenomena may influence the bond strength during the annealing treatment. First, annealing is used to reduce residual stresses between the solid-state bonded dissimilar materials (Chang & Jha 2003). Second, according to the phase diagrams of the interface components (Fe,Cu,Zn,Cr), no intermetallic phase forms between St13 and MS90 alloy, enhancement of the bond strength after annealing may be related to the atomic diffusion at the interface (Peng et al. 1999). Other researchers (Vaidyanath et al. 1959, Wright et al. 1978, Bay et al 1986, Zhang & Bay, 1997) have developed some macroscopic theoretical models for roll bonding. For instance, Vaidyanath et al. have proposed the following equation for predicting bonding quality (Vaidyanath, 1959):

$$S_w = S_m.R_f(2 - R_f) \tag{2}$$

where S_w is the strength of the bonds, S_m is the strength of base metal, and R_f is the final reduction at the end of rolling pass.

In this research, with attention to microscopic details, the total bond strength was presented by summation of the strength of each mechanism according to the following equation:

$$S = S_b F_b + S_c F_c \tag{3}$$

where S is the total bond strength, S_b is the bond strength of the blank bond, S_c is the bond strength of the block bond, F_b is the area fraction of the blank bond and F_c is the area fraction of the block bond. The area fractions of blank and block areas are given by Eqs. (4) and (5):

$$F_b = A_b/A \tag{4}$$

$$F_c = A_c/A \tag{5}$$

where A is the overall bonded area, and A_b and A_c are the blank bond area and the block bond area, respectively. In order to determine F_b and F_c, the contribution of the narrow transverse blanks, which where paralleled to rolling direction, on the strength was ignored. Considering the longitudinal blanks were perpendicular to rolling direction, the following equations can be used for calculation of the fraction of blank and block areas:

$$F_b = L_b/L \tag{6}$$

$$F_c = L_c/L \tag{7}$$

$$F_b + F_c = 1 \tag{8}$$

where L is the total length of the interface in rolling direction, L_b the average length of width of blank area and L_c the average of block area in rolling direction on the top of the chromium interlayers. These lengths are shown schematically in Fig. 12. L, L_b and L_c were measured by the following equations:

$$L = L_b + L_c \tag{9}$$

$$L_b = \sum_{i=1}^{n} l_{bi} \tag{10}$$

$$L_c = \sum_{i=1}^{n} l_{ci} \tag{11}$$

where i is the number of any individual chromium block or blank along the length L. The average number of l_{bi} and l_{ci} which were taken as 30. Fig. 13 shows for a total thickness reduction of 40% the area fraction of the blank bond

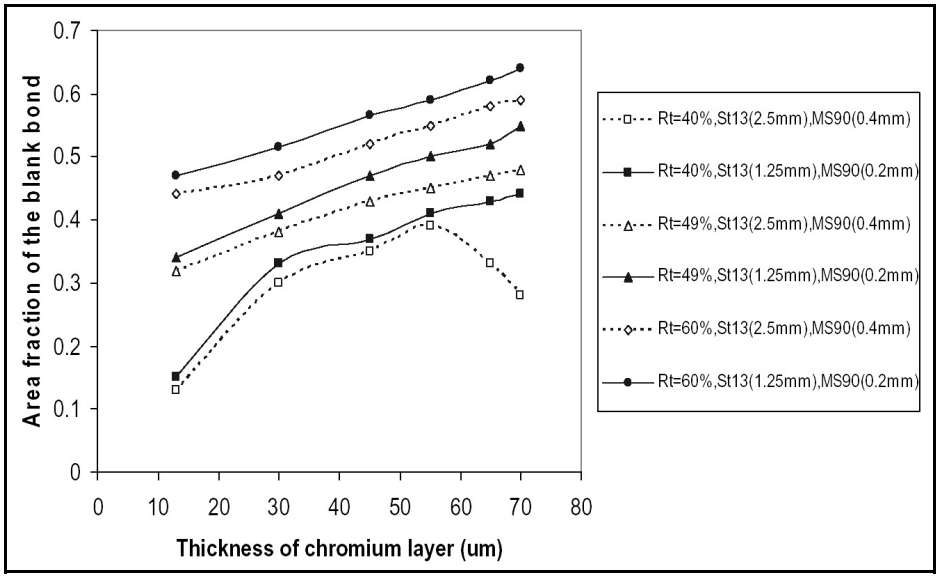

Figure 13. Variation in area fraction of blank bond with the thickness of the coating layer for different thickness reductions and initial thicknesses

increased with increasing the interlayer thickness up to 55μm, and then decreased. Whereas for total reduction of 49% and more the increasing trend of blank bond area fraction continued with increasing thickness of coating layer. Although, variation of area fraction of the blank bond in lower initial thickness (i.e.,St13 (1.25mm), MS90 (0.2mm)) was always higher with an intensified trend. On the other hand, analytical models of the cold roll bonding predict that by increasing the thickness reduction, the initial bonded areas shift to the entrance of the roll gap (Yong et al. 2000, Tzou & Huang, 2003). It means that the time of loading by normal pressure on the MS90/St13 interface becomes longer and thus, the bonding can be established easier. Meanwhile, the results related to the effect of initial thickness of the sheets on the bond strength may be attributed to the following:

(a) When the initial thickness of the sheets reduces, the required pressure to reach a certain reduction may increase (Hosford & Caddell, 1983), (b) Also the position of bonding point approaches to the entrance of the roller gap at a certain reduction, when the initial thickness of the sheets reduces (Tzou & Huang, 2003).

In a constant thickness reduction, it is reported that mean contact pressure increases with decreasing the thickness of core layer despite the falling of rolling force (Tzou & Huang 2003, Huang et al. 2003 & Yong et al. 2000). This has been attributed to the decreasing of roll-strip contact length (Tzou 2001), since the effect of decrease in strip-roll contact length dominates the effect of decrease in rolling force and results to increasing of mean contact pressure. The extended relative bonding length, which is caused by internal layer thickness reduction, can be originated from the point that clad layer strain increases with decreasing the thickness of the core layer, therefore by paying attention to the point that the bond creation between layers can be more affected by the soft layer deformation (Pendrous 1984), higher deformation of clad layer can causes an increase in the number of virgin metal overlapping places for bond creation. Consequently, it results to lowering the threshold thickness reduction to establish the bonding between layers (Pendrous 1984).

The total bond strength can also be represented by the following equation (derived from Eqs. (3) and (8)):

$$S = (S_b - S_c)F_b + S_c \tag{12}$$

On the base of the above formula, there should be a linear relationship between S and F_b, so that by increasing F_b, S will be increased. The measured variation in bond strength with the area fraction of the blank bond for the best MS90/St13 composite sheet is shown in Fig. 14. When the bonded area

considered entirely due to block bonds, the value of F_b becomes 0, and S becomes equal to S_c. Similarly, when the bonded area considered entirely due to blank bonds, F_b will be 1, and S becomes equal to S_b.

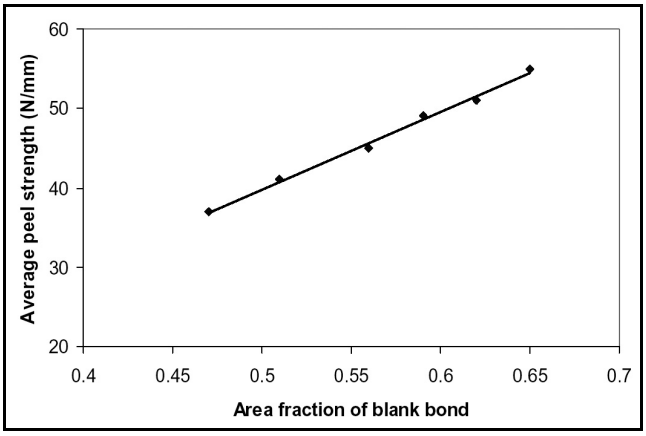

Figure 14. The linear relationship between bond strength and area fraction of blank bond

Consequently from this figure, S_b and S_c were found to be equal to 154.28 and 30.41 N, respectively. Thus, the bonding strength of the blank bond is nearly five times greater than that of the block bond, and the total bond strength was principally dependent on the bond strength and the area fraction of the blank bond.

Fig. 11 confirms the existence of the bonds between the two layers in the blank regions, as a large amount of Fe particles were detected on the peeled surface of MS90 layer. On the other hand, because of difference in flow velocity of brass and steel layers a rotational momentum can be induced, so that the blocks rotated about $\Theta = 45$ degrees which provide the lower area of blanks for the material extruding into the blank areas (Fig. 12). The thicker the chromium layer, the larger the angle of rotation (Θ) is, and therefore the interlayer blocks can take over a much more bonded interface. Thus, as a result of this rotation the area fraction of the blank bond decreases ($F_b = 1 - F_c/Cos\Theta$). Meanwhile, by increasing the coating thickness, the actual dimension ratio (t/w) of the blocks exceeded from an optimum value, 55μm, so that the extrusion of MS90 layer into the blank area become incomplete. However, the increasing of thickness reduction more than 49% differs the bonding strength variation trend by the means of blocks distance increment (Fig. 8). Indeed, the effect of rising of coating thickness more than its optimum content and rotation of the blocks were negligible (Fig. 6), especially for low initial thickness of the sheets (Fig. 13). Nevertheless in this study, one can claim that dominant mechanism of bonding

the interface of the sheets was the bonding within the blank regions. In other words, the metallurgical bonds between the exposed areas of steel sheet and the extruded brass during rolling reduction provided the major bonding mechanism of the sheet composite. Finally, the results of this research shows that the contribution of metallurgical bonding between extruded brass and steel virgin metals is dominant when compared to the mechanical locking by block constraints. However, one should have in mind that the strength of a metallurgical bonding influenced by annealing treatment. So, for a high bonding strength the more rolling operation is not enough and annealing is required. Accordingly, the conditions strength and degree of importance of the variables can be established. This information can be useful in producing of different multi-layered composites prepared by coating interlayer during various deformation processes. Although, more comprehensive investigations is required for better understanding of the role of each bonding mechanism in overall strength of bonding and dominant variables in different settings.

CONCLUSIONS

1 - Bonding MS90 alloy and chromized St13 steel sheets required a threshold rolling reduction of at least 36%, but the overall bond strength decreased by increasing the chromium coating thickness more than 55μm for the total thickness reduction less than 54%.

2 - The strength of the bonds within the blank area was five times greater than the strength of the block bonds. This means that the total bond strength depends basically on the metallurgical bond strength and the area fraction of the blank bond.

3 - Since the dominant mechanism of bonding was the metallurgical bonding in blank areas, therefore a total reduction and a coating thickness can be considered as optimum conditions which provide the maximum bonding strength. The optimum conditions for this study obtained at 63% total thickness reduction and coating thickness of 55μm.

4 - The annealing treatment and reduction in initial thickness of both St13 steel and MS90 sheets causes to improve the bond strength and decreases the threshold reduction.

REFERENCES

Alizadeh, M. & Paydar, M.H. 2009. Study on the effect of presence of TiH2 particles on the roll bonding behavior of aluminum alloy strip. Materials and Design, **30**: 82-86.

Al-Sharee dah, E. 2008. Treatment of multi-layered composite structures using the undetermined multipliers method. Kuwait Journal of Science and Engineering, **35**: -.

Bay, N. 1986. Cold pressure welding; characteristics, bonding mechanism, bond strength. Journal of Metal Construction, **18(8)**: 369-372.

Bay N. 1986. Cold welding1 Characteristics, bonding mechanism, bond strength. Metal Construction, **18(8)**: 369-372.

Butlin, I.J. & Mackay, C.A. 1979. Experiment on the roll-bonding of tin coatings to non-ferrous substrates. Sheet Metal Industry, **11**: 1063-1072.

Casolo, S.R., Negrete. Sanchez, J, Lopez Parra, M & Torres-Villasenor,G. 2007. Analysis of the behavior of a clad material Al-Zinag-Al. Materials Science Forum, **551-552**: 337-340.

Cave, J.A. & Williams, J.D. 1973. The mechanism of cold pressure welding by rolling. Journal of the Institute of Metals, **101(8)**: 203-207.

Chang, C.S. & Jha, B. 2003. Application of roll welding to brazing. Welding Journal, 82(10): 28-31.

Clemensen, C. & Julstarp, O. 1986. Cold welding: Influence of surface preparation on bond strength, Journal of Metal Construction, **18(10)**: 625-629.

Danesh Manesh, H. & Karimi Taheri, A. 2003. Bond strength and formability of an aluminum-clad steel sheet, Journal of Alloys and Compounds, **361:** 138- 143.

Danesh Manesh, H. & Shahabi, H.Sh. 2008. Effective parameters on bonding strength of roll bonded Al/St/Al multilayer strips, Journal of Alloys and Compounds, In Press.

EI-Mahallawy, N.A., Shady, M.A. & EI-Sissi, A.R. 1997. Analysis of coating layer formed on steel strips during aluminizing by hot dipping in Al-Si baths. Material Science Technology, **13**: 832-840.

Granjun, H. 1991. Fundamentals of Welding Metallurgy. Cambridge Abington Publishing.

Hosford, W.F. & Caddell, R.M. 1983. Metal Forming. Prentice-Hall, Englewood Cliffs, New Jersey.

Hwang, Y.M., Hsu, H.H. & Lee, H.J. 1995. Analysis of sandwich sheet rolling by stream function method. International Journal of Mechanical Sciences, **37(3)**: 297-315.

Huang, M.N., Tzou, G.Y. & Syu, S.W. 2003. Investigation on comparisons between two analytical models of sandwich sheet rolling bonded before rolling. Journal of Materials Processing Technology, **140:** 598-603.

Kang, C.G. & Kwon, H.C. 2002. Finite element analysis considering fracture strain of sheath material and die lubricant in extrusion process of Al/Cu clad composites and its experimental investigation. International Journal of Mechanical Sciences, **44**: 247-267.

Karimi Taheri, A. 1993. Analytical study of drawing of non-bounded trimetallic strips. International Journal of Machine and Tools Manufacturing, **33(1)**: 71-88.

Kreye. H. & Thomas K. 1977. Electron microscopically test and bonding mechanism of cold pressure welding. Journal of Welding and Cutting. **29**: 249-252.

Lee, J.E., Bae, D.H., Chung, W.S., Kim, K.H., Lee, J.H. & Cho, Y.R. 2007. Effects of annealing on the mechanical and interface properties of stainless steel/aluminum/copper clad-metal sheets. Journal of Materials Processing Technology. **187-188**: 546-549.

Masahashi, N, Komatsu, K, Kimura, G., Watanabe, S & Hanada, S. 2006. Fabrication of iron aluminum alloy/steel laminate by clad rolling. Metallurgical and Materials Transactions. **37A**: 1165-1673.

Pan, D., Gao, K. & Yu, J. 1989. Cold roll bonding of bimetallic sheets and strips. Material Science and Technology, **5**: 934-939.

Pendrous, R.C. 1984. Ph.D. Thesis, The University of Leeds.

Peng, X.K., Heness, G.I. & Yeung, W. 1999. Effect of rolling temperature on interface and bond strength development of roll bonded copper/aluminium metal laminates. Journal of Material Science, **34**: 2029-2038.

Quadir, M.Z., Wolz, A., Hoffman, M. & Ferry, M. 2008. Influence of processing parameters on the bond toghness of roll-bonded aluminum strip. Scripta Materilia, **58**: 959-962.

Soltan Ali Nezhad, M. & Haerian Ardakani, A. 2009. A study of joint quality of aluminum and low carbon steel strips by warm rolling. Materials and Design, **30**: 1103-1109.

Thomas, K. & Petri, M. 1994. Roll Welding. In: ASM Welding Handbook, Pp.312-314.

Tylecote, R. 1968. The solid phase welding of metal. Edward Arnold Publishers, London.

Tzou, G.Y. & Huang, M.N. 2003. Analytical modified model of the cold bond rolling of unbounded double-layers sheet considering hybrid friction. Journal of Material Processing Technology, **140**: 622-627.

Tzou, G.Y. 2001. The theoretical study on the cold sandwich sheet rolling considering coulomb friction. Journal of Materials Processing Technology, **114**: 41-50.

Vaidyanath, L.R., Nicholas, M.G. & Milner, D.R. 1959. Pressure Welding by Rolling. British Welding Journal, **6**: 13-28.

Wright, P.K., Snow, D.A. & Tay, C.K. 1978. Interfacial conditions and bond strength in cold pressure welding by rolling. Metals Technology, **5(1)**: 24-31.

Yong, J., Dashu, P., Dong, L. & Luoxing, L. 2000. Analysis of clad sheet bonding by cold rolling. Journal of Material Processing Technology, **105**: 23-37.

Yongbing, L., Jian, A. & Darn, S. 2000. Interfacial bonding strength of Al-Pb bearing alloy strips and hot dip aluminized steel sheets by hot rolling. Transactions of Nonferrous Metals Society of China, **10:** 625-631.

Yong, J., Dashu, P., Dong, L. & Luoxing, L. 2000. Investigation on comparisons between two analytical models of sandwich sheet rolling bonded before rolling. Journal of Materials Processing Technology, **105**: 32-37.

Zhang, W. & Bay, N. 1997. Cold welding-Theoretical modeling of the weld formation. Welding Journal, **76 (10)**: 417-420.

Zhang, W. & Bay, N. 1986. Cold welding: Theoretical modeling of the weld formation, Welding Research Supplement, **12**: 417-420.

Submitted : *22/6/2008*
Revised : *3/5/2009*
Accepted : *28/5/2009*

تأثير الكروم على ميكانزم الربط في صفيحة المركب CuZn10–فولاذ–CuZn10

بهزاد الطولم نزاد[1] و حسين العرب[1و2]

[1] مدرسة علوم المواد والتكنولوجيا، جامعة إيران للعلوم والتكنولوجيا، نارماك- طهران - إيران
[2] مركز الجودة للمواد المتطورة والتقنيات btolaminejad@iust.ac.ir

خلاصة

هذا المقال يتحدث عن تأثيرالدرفلة على قوة الربط في صفيحة مركب ناتج من رقائق الخليط MS90 (CuZn10) وصفائح الفولاذ الكرومية St13 الصلبة. الكروم الصلب المطبق على سطح صفائح الفولاذ تفاعل كطبقة بينية رابطة. لاحظنا أن الربط بين هذين المعدنين ناتج عن نوعين مختلفين من الروابط: روابط المجموعة بين رقائق MS90 وطبقة التغليف الفوقية الكرومية الجزئية، والروابط الفارغة بين MS90 وسطح الفولاذ في منطقة الطبقة الجزئية الكرومية. بالإضافة،قمنا بدراسة تأثير وقت التغليف على سمك طبقات التغليف الناتجة عن مختلف المناطق الجزئية للروابط الفارغة خلال الدرفلة على قوة الربط في صفيحة المركب. إنقاص السمك الإبتدائي للصفيحة والمعالجة الحرارية بعد الدرفلة يحسن من قوة الربط. لاحظنا علاقة خطية بين قوة الربط والمنطقة الجزئية للروابط الفارغة.